Experimental Mechanics (2014) 54:1491–1495
DOI 10.1007/s11340-014-9917-8

BRIEF TECHNICAL NOTE

Accurate Stiffness Measurement of Ultralight Hollow Metallic Microlattices by Laser Vibrometry

L. Salari-Sharif · L. Valdevit

Received: 18 September 2013 / Accepted: 19 June 2014 / Published online: 15 August 2014

Abstract Recent progress in advanced manufacturing enables fabrication of macro-scale hollow metallic lattices with unit cells in the millimeter range and sub-unit cell features at the submicron scale. If designed to minimize mass, these metallic microlattices can be manufactured with densities lower than 1 mg/cm3, making them the lightest metallic materials ever demonstrated. Measuring the compressive stiffness of these ultralight lattices with conventional contact techniques presents a major challenge, as the lattices buckle or locally fracture immediately after contact with the loading platens is established, with associated reduction in stiffness. Non-contact resonant approaches have been successfully used in the past for modulus measurements in solid materials, at both small and large scales. In this work we demonstrate that Laser Doppler Vibrometry coupled with Finite Elements Analysis is a suitable technique for the reliable extraction of the Young's modulus in ultralight microlattices.

Keywords Metallic microlattices · Young's modulus · Laser doppler vibrometry · Natural frequency · Finite element simulation

Recent progress in advanced manufacturing enables fabrication of macro-scale hollow metallic lattices with unit cells in the millimeter range and sub-unit cell features at the submicron scale. If designed to minimize mass, these metallic microlattices can be manufactured with densities lower than 1 mg/cm^3, making them the lightest metallic materials ever demonstrated [1–3]. Measuring the compressive stiffness of these ultralight lattices with conventional contact techniques presents a major challenge, as the lattices buckle or locally fracture immediately after contact with the loading platens is established, with associated reduction in stiffness. Non-contact resonant approaches have been successfully used in the past for modulus measurements in solid materials, at both small [4–7] and large scales [8–10]. In this work we demonstrate that Laser Doppler Vibrometry [11, 12] coupled with Finite Element Analysis is a suitable technique for the reliable extraction of the Young's modulus in ultralight microlattices.

Ultralight nickel hollow microlattices (Fig. 1) were fabricated as described in [1], and glued to carbon/epoxy face sheets using Epoxi-Patch Adhesive glue, resulting in a sandwich configuration. The planar face sheets are essential for reliable laser surface tracking. All sample dimensions are reported in Table 1. All vibrometry measurements were performed with a Polytec Micro Systems Analyzer (MSA-500), a fully integrated structural dynamics system. This instrument enables real-time, non-contact in-plane and out-of-plane vibration analysis (only the latter is used in this work). From the detection of resonant frequencies, the effective Young's modulus, *E,* of the sample in the direction normal to the face sheets can be obtained by close-form analytical solutions or fitting to Finite Element models. To verify the accuracy of this approach, an aluminum cantilever bar (E=69 GPa) was excited acoustically and the first two resonant modes were measured at 409 kHz and 2,560 kHz. The Young's modulus, *E,* was extracted from the analytical expression of the resonant frequency of each mode *n*, $f_{(n)} = \frac{\alpha_{(n)}^2}{2\pi}\sqrt{\frac{EI}{\rho AL^4}}$, where *I*, *A* and *L* are the moment of inertia, the area and the length of the beam, respectively, ρ is the density of the material, and $\alpha_{(1)}$=1.875 and $\alpha_{(2)}$=4.694 ($\alpha_{(n)}=k_{(n)}L$, with $k_{(n)}$ the wave number associated to the nth vibration mode) [13]. The modulus extracted from the first two modes was *E= 68.6 GPa* and *E= 68.4 GPa*, respectively. The consistency between the two measurements and the agreement with the known value for aluminum demonstrate the robustness of the approach.

L. Salari-Sharif · L. Valdevit (✉)
University of California, Irvine, Irvine, CA 92697, USA
e-mail: valdevit@uci.edu

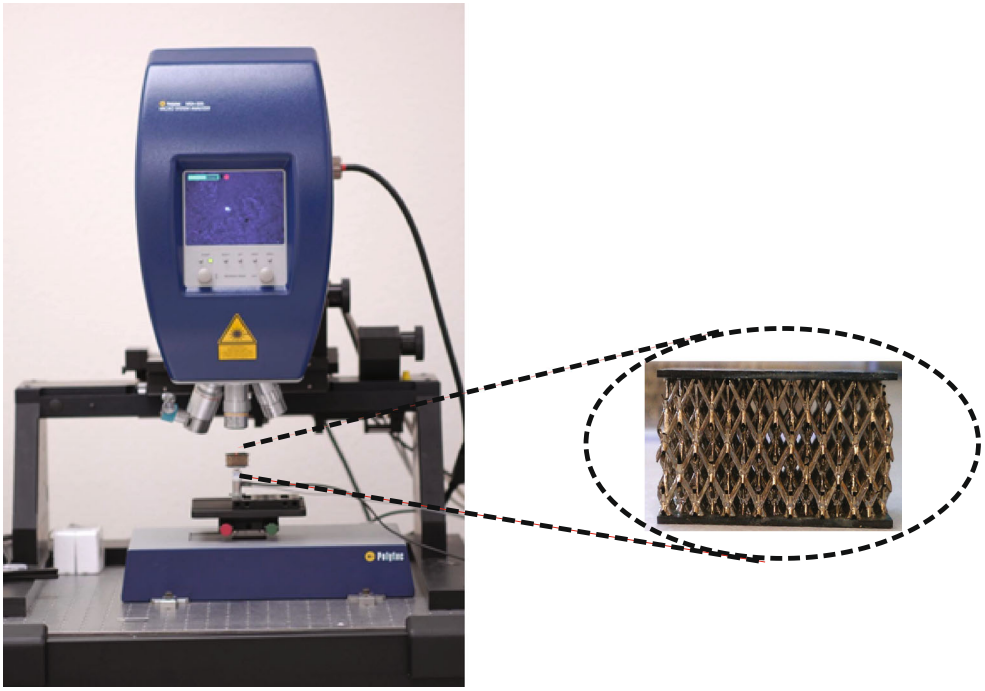

Fig. 1 The experimental setup, with the microlattice sandwiched between carbon-epoxy face sheets. The bottom face is excited by a piezo-actuator, whereas the velocity of the top face is detected in non-contact mode *via* a Laser Doppler Vibrometer (Polytec MSA-500)

The microlattice sandwich samples were mounted on a piezoelectric actuator with a travel range of 15 μm. The actuator excited the sample from one side in the direction normal to the face sheet; the actuation was sinusoidal, with frequency swept in the 0–4 kHz range. The velocity of the opposite face sheet along the same direction was measured by scanning laser vibrometry. Multiple points on the face sheet were scanned, to capture the three-dimensional movement of the sample (and hence enable the identification of the different modes). The instrument and the test configuration are shown in the inset in Fig. 1.

The response of sample C (Table 1) is shown in Fig. 2(a). For this sample, two eigenmodes were detected within the excitation range at 1,746 Hz and 2,302 Hz.

Finite element simulations (frequency extraction – linear perturbation analyses) were performed in ABAQUS/Standard to extract the relation between the Young's modulus and the natural frequencies. The sample was modeled as an effective isotropic solid core within two perfectly bonded face sheets. 8-node linear solid elements (C3D8R) were used for both materials. At least 30 nodes were seeded along the core edges and 4 across the face sheets. The density of the core was determined by weighing the microlattice sample and dividing the mass by the bounding volume. As the Poisson's ratio, ν, of these lattices is difficult to measure, selected Finite Element simulations were performed with $\nu=0$ and $\nu=0.5$. For all cases, the difference in the natural frequencies was~10 %, inducing a change in the predicted Young's modulus of less than 12 %, and hence generally negligible. Consequently, a Poisson's ratio of 0.3 for the core was assumed for all subsequent calculations. The effective Young's modulus of the solid core was swept within a reasonable range, chosen based on analytical estimates according to the sample density [14]. The six lowest vibration modes and corresponding eigenfrequencies were obtained *via* eigenvalue extraction. The effect of the Young's modulus of the core on the natural frequencies for the first six modes is depicted in Fig. 2(b). The first and second modes involve primarily shear motion in the xy plane, along the x and y directions, respectively (z being the out-of-plane axis

Table 1 Summary of dimensions and properties of tested microlattices and face sheet materials. (All the face sheets were made of carbon-epoxy laminates, with thickness of 0.78 mm and elastic modulus of ~150 GPa)

Sample	Wall thickness t (μm)	Strut diameter D (μm)	Strut length L (μm)	Strut angle (°)	Thickness to diameter ratio	Density (kg/m^3)	Relative Density (%)	Face sheet mass (mg)	Relative face sheet to core mass ratio
A	1±0.1	560±30	4600±120	60±2	$(1.8\pm0.3)\times10^{-3}$	7.66±0.7	0.086±0.01	500	9.8
B	0.53±0.06	460±20	1743±36	55±2	$(1.1\pm0.2)\times10^{-3}$	8.82±0.8	0.09±0.01	475	10.5
C	1.2±0.12	560±30	4600±120	60±2	$(2.1\pm0.4)\times10^{-3}$	10.05±1	0.11±0.02	475	8
D	0.56±0.03	115±9	1050±32	60±2	$(4.8\pm0.6)\times10^{-3}$	18.22±1.8	0.21±0.03	283	11.3
E	4±0.4	430±15	4000±120	60±2	$(9.3\pm0.7)\times10^{-3}$	28.95±2.9	0.33±0.04	334	4

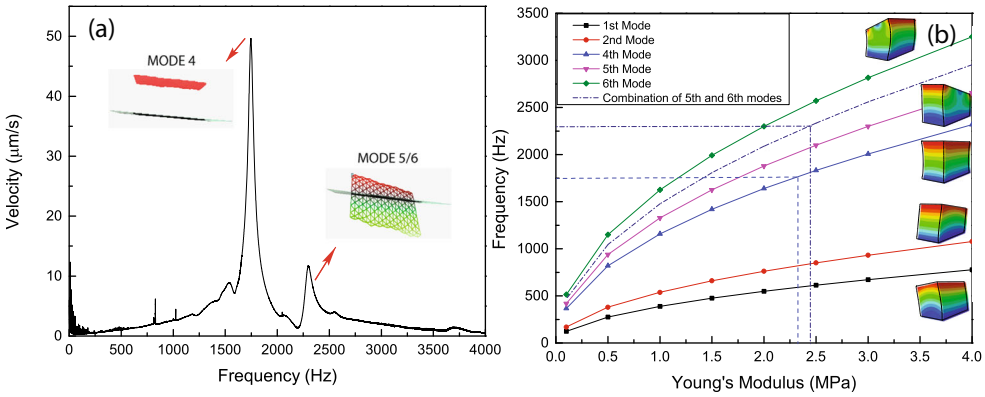

Fig. 2 a) Frequency response of a sandwich panel with ultralight micro-lattice core, captured by Laser Doppler Vibrometry. The mode shapes are displayed. b) Natural frequencies of a sandwich panel with homogenized core, as a function of the Young's modulus of the core (from Finite Element analysis). The mode 4 peak in (**a**) can be used in (**b**) to extract the modulus E_z of the core

for the sandwich configuration). As the z-displacement is not identically zero, they are reported in Fig. 2(b) for completeness; however, they are generally undetectable with z-direction actuation/detection. The third mode is a twist about the z-axis, and does not contain any z-component of displacement; as such, it is undetectable with out-of-plane vibrometry and is not included in the figure. The fourth mode is the classic extensional mode. Finally, the fifth and sixth modes are combination of extensional and bending modes about the X and Y axes, with displacement primarily in the z-direction. In the experiments, these two modes appeared combined, as indicated by the X and Y components of the rotation axis of the top face sheet (see inset in Fig. 2(a)). Hence, an average curve was added to the numerical results (dotted line in Fig. 2(b)).

It is important to notice that the microlattices under consideration are orthotropic. If the x and y directions are equivalent, six elastic constants would be needed to fully characterize the elastic response of the material. As the presence of the face sheets (essential for optical detection) and the single-axis detection limit the number of modes that can be observed, fitting the entire elastic tensor to the observed peaks presents significant challenges. Here we concern ourselves with the determination of the Young's modulus in the z direction (which is one of the critical engineering properties for lattice materials). As the fourth mode depends almost exclusively on E_z, its detection and identification allows extraction of the modulus. Once E_z is extracted, the modeling/experiment agreement on the frequency of other detected modes provides some information on the deviation from isotropy. For the sample depicted in Fig. 2(b) (Sample C in Table 1), the modulus E_z extracted from the experimentally measured mode 4 frequency (Fig. 2(a)) is 2.3 MPa. As modes 5 and 6 also depend almost exclusively on E_z, a fitting from the mode 5/6 peak would result in a modulus prediction that is fairly similar (~7 % larger). Fitting on higher modes that involve other elastic moduli would obviously not provide realistic results, unless the lattice under investigation was isotropic. In conclusion, this approach provides a simple methodology to calculate the modulus in a single direction *via* a non-contact technique that allows detection and identification of the suitable mode (mode 4) or combination of modes.

The Young's modulus of micro-lattice materials extracted with this technique is compared to FE results presented elsewhere [14] (Fig. 3) and conventional measurements obtained with a universal test frame. In the experiments, the moduli were extracted from the slope of the stress–strain curve upon unloading from 50 % strain. No face sheets were applied to the specimen, although separate measurements with face sheets only showed a 10 % modulus increase. All samples exhibit relative density between 0.08 and 0.32 %. The ABAQUS/Standard solver was used for all FE simulations. All simulations were performed on single unit cells, meshed with a dedicated geometry modeling code [14–16] (Fig. 4), using 4-node shell elements (S4). Notice that these FE analyses are very different from those used for the extraction of the Young's modulus of the lattice (Fig. 2(b)): while those were solid models of an effective cellular medium, in this case a single unit cell of the truss lattice is meshed with shell elements. Two different boundary conditions were used: fully periodic BCs, and free-edge BCs. In the latter, no translational or rotational constraint is imposed along the sides of the unit

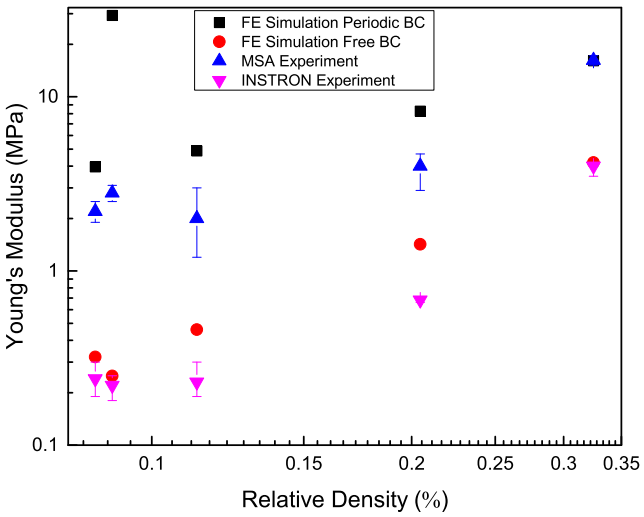

Fig. 3 Comparison of experimental results and Finite Element simulations for the compressive modulus of ultralight micro-lattices. Notice that Laser Doppler Vibrometry (MSA) captures moduli that are consistently ~5–10× larger than provided by conventional compression (Instron) tests

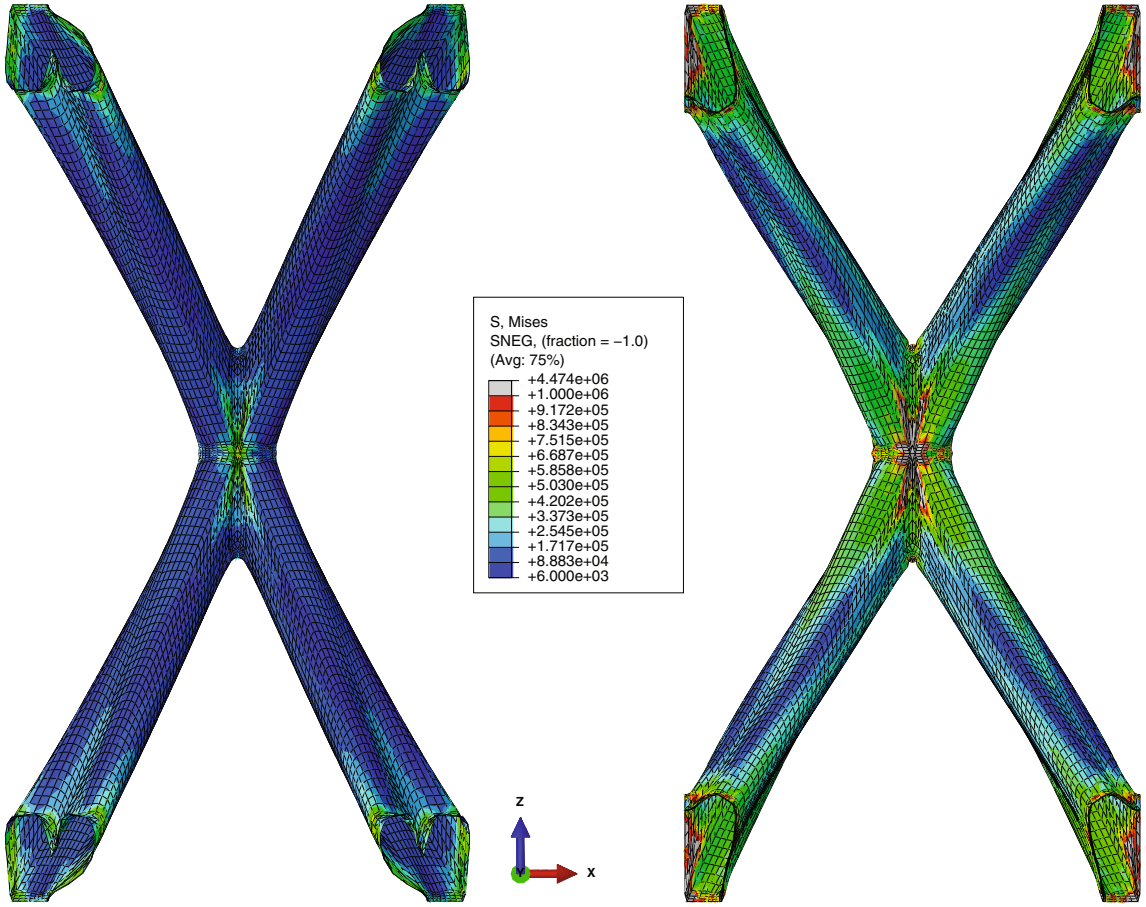

Fig. 4 The insets represent contours of the Von Mises stress in Finite Element simulations of sample C (Table 1) under 1 % compression strain, with free edge (left) and periodic (right) boundary conditions

cell [14, 15], simulating a deformation process where each cell is only minimally constrained by the adjacent cells (*e.g.*, as a consequence of local buckling or fracture events at the nodes [3]). Fig. 4 displays contours of Von Mises stress, for the same lattice under the same applied external strain, for the two different boundary conditions. Much higher stress levels are noticeable for the periodic boundary conditions, indicating higher strain energy (and higher stiffness). Notice that as expected, the free-edge BC localizes the strain energy at the nodes with the bars carrying minimal stress. As shown in Fig. 3, the difference in modulus prediction between the two BCs can be in excess of an order of magnitude. The results of conventional stiffness measurements performed upon unloading with a universal (Instron) test frame (Fig. 3) result in Young's moduli even lower than predicted by the free-edge BC simulations, generally by a factor 2–3. This is attributed to the fact that the necessary load application results in the characterization of a post-buckled or post-fractured lattice, which can easily be an order of magnitude more compliant than the pristine material. Although the free-edge BCs limit the constraining effects of the neighboring cells to a minimum (hence mimicking some nodal fracturing and buckling), the simulations nonetheless model a pre-buckled unit cell. Importantly, traditional Instron measurements provide moduli that are more than an order of magnitude lower than those predicted by FE simulations with periodic boundary conditions (the typical BC of choice for periodic materials). Conversely, the vibrometry measurements presented in this article are generally ~5–10 times higher than the Instron measurements, and approach the simulation results obtained with fully periodic BCs (generally within a factor of 2, with the exception of sample B, $\overline{\rho}= 0.09\%$, for which the experimental result is 10 times lower than the FE result; we surmise that this is due to its "stubby" geometry, see Table 1[1]). This confirms that non-contact vibrometry allows extraction of moduli of a pristine structure, without introducing damage during the measurement. The factor of 2 discrepancy with the simulations can be attributed to deviations from the idealizations assumed in the simulations (in particular the

[1] A stubby geometry, with a very low L/D ratio, is heavily affected by the boundary conditions, as a significant fraction of the bar nodes are on the boundary. Fully constraining all the boundary nodes against rotations, and imposing a symmetric deformation, results in excessive stiffening, as in practice minor rotations between cells can occur. Furthermore, stubby geometries are more affected by the details of the nodal fillets, which are difficult to capture exactly.

assumption that all unit cells deform identically), and to manufacturing imperfections.

In conclusion, we showed that contact measurement techniques are not applicable to Young's modulus measurements on ultralight cellular materials with deformation governed by localized buckling and/or fracture events, as the necessary load application results in the characterization of a post-buckled or post-fractured lattice. In this note, we demonstrated that a combination of non-contact scanning vibrometry experiments and Finite Element simulations yields values of the Young's modulus that are as much as 10 times higher than those obtained by traditional compression tests, and close to those predicted by FE simulations with periodic boundary conditions. As these BCs correctly capture the symmetry of the sample and loading conditions and predict a compatible deformation field (unlike the free-edge BCs in good agreement with the compression test results), we conclude that the proposed technique significantly increases the accuracy of the measurement. With fabrication of additional samples, all the three Young's moduli of an orthotropic lattice material can be obtained. A similar approach based on in-plane detection can be used for the extraction of shear moduli.

Acknowledgments This work was financially supported by the Office of Naval Research under Grant No.N00014-11-1-0884 (program manager: D. Shifler). This support is gratefully acknowledged. The authors are also thankful to Tobias Schaedler, Alan J. Jacobsen, William B. Carter of HRL Laboratories for providing samples and for useful discussions.

References

1. Schaedler TA, Jacobsen AJ, Torrents A et al (2011) Ultralight metallic microlattices. Science 334:962–965
2. Maloney KJ, Roper CS, Jacobsen AJ, et al. (2013) Microlattices as architected thin films: Analysis of mechanical properties and high strain elastic recovery. APL Materials 1:022106–8
3. Torrents A, Schaedler TA, Jacobsen AJ et al (2012) Characterization of nickel-based microlattice materials with structural hierarchy from the nanometer to the millimeter scale. Acta Mater 60:3511–3523
4. Cleveland JP, Manne S, Bocek D, Hansma PK (1993) A nondestructive method for determining the spring constant of cantilevers for scanning force microscopy. Rev Sci Instrum 64:403–405
5. Kiesewetter L, Zhang J-M, Houdeau D, Steckenborn A (1992) Determination of young's moduli of micromechanical thin films using the resonance method. Sensors Actuators A Phys 35:153–159
6. Chopra NG, Zettl A (1998) Measurement of the elastic modulus of a multi-wall boron nitride nanotube. Solid State Commun 105: 297–300
7. Qin Q, Xu F, Cao Y et al (2012) Measuring true young's modulus of a cantilevered nanowire: effect of clamping on resonance frequency. Small 8:2571–2576
8. ASTM E1875−08 (2013) standard test method for dynamic young's modulus, shear modulus, and poisson's ratio by sonic resonance.
9. ASTM E1876−09 (2013) standard test method for dynamic young's modulus, shear modulus, and poisson's ratio by impulse excitation of vibration.
10. Ritchie IG (1973) Improved resonant bar techniques for the measurement of dynamic elastic moduli and a test of the timoshenko beam theory. J Sound Vib 31:453–468
11. Righini GC, Tajani A, Cutolo A (2009) An introduction to optoelectronic sensors. Hackensack, NJ
12. Castellini P, Martarelli M, Tomasini EP (2006) Laser Doppler Vibrometry: Development of advanced solutions answering to technology's needs. Mech Syst Signal Process 20:1265–1285
13. Meirovitch L (1967) Analytical methods in vibrations. Macmillan, New York
14. Godfrey SW, Schaedler TA, Jacobsen AJ et al (2014) Optimal design of stiff and light hollow microlattices. Materials and Design, Submitted
15. Valdevit L, Godfrey SW, Schaedler TA et al (2013) Compressive strength of hollow microlattices: experimental characterization, modeling, and optimal design. J Mater Res 28(17):2462–2473
16. 16. Godfrey SW, Valdevit L (2012) A novel modeling platform for characterization and optimal design of micro-architected materials. Proceedings AIAA SDM Conference, pp. 2003–2012